

# β-Band Correlates of the fMRI BOLD Response

Claire M. Stevenson,\* Matthew J. Brookes, and Peter G. Morris

*Sir Peter Mansfield Magnetic Resonance Centre, School of Physics and Astronomy, University of Nottingham, University Park, Nottingham, NG7 2RD, United Kingdom*

---

**Abstract:** Oscillatory activity in the  $\beta$ -band (15–30 Hz) has been studied in detail in the sensorimotor cortex. It has been postulated that  $\beta$ -activity acts as a localized gating of cortical activity. Here, the induced oscillatory response in the  $\beta$ -band is measured by magnetoencephalography, and the hemodynamic response is measured by fMRI. We assess the linearity of the responses to stimuli of varying duration in the primary motor cortex and to a sinusoidal drifting grating of varying contrast amplitude and drift frequency in the visual cortex. In this way, we explore the nature of  $\beta$ -oscillations and their relationship with hemodynamic effects. Excellent spatial colocalization of BOLD and  $\beta$ -activity in both central and lateral (MT) visual areas and sensorimotor areas suggests that the two are intimately related. In contrast to the BOLD response, the level of  $\beta$ -desynchronization is not modulated by stimulus contrast or by stimulus duration, consistent with a gating role. The amplitude of  $\beta$ -desynchronization in the central visual area is however modulated by drift frequency, and this seems to parallel the modulation in BOLD amplitude at the same location. *Hum Brain Mapp* 32:182–197, 2011. © 2010 Wiley-Liss, Inc.

**Key words:** MEG; fMRI; oscillatory activity; beta band; contrast response; linearity

---

## INTRODUCTION

The noninvasive functional neuroimaging techniques, PET, and, more recently, fMRI [Bandettini et al., 1992; Kwong et al., 1992; Ogawa et al., 1990] have been of enormous benefit in the study of human brain function. Yet neither are direct measures of brain activity, and the most widely applied method, BOLD fMRI, is governed by multiple factors, including, changes in cerebral blood flow (CBF), cerebral blood volume (CBV), blood oxygen extraction, and local metabolism driven by neural activity. The precise nature of the coupling mechanism between the hemodynamic response measured by BOLD fMRI and

the underlying neural activity is poorly understood and remains an area of intense research activity [Fox and Raichle, 1986; Heeger and Ress, 2002; Maloney and Grinvald, 1996; Maloney et al., 1997]. In contrast, electroencephalography (EEG) and magnetoencephalography (MEG) do provide direct measures of neural activity, but source localization is challenging. To generate a measurable electric potential or magnetic field requires the synchronous activity of a large number of neurons. This synchronicity may be elicited in response to a stimulus (evoked response) or may be one of the brain's natural rhythms, noted in the earliest EEG studies [Berger, 1929] and omnipresent, but whose significance remains unclear. There are clear merits in multimodal approaches: the techniques will have complementary strengths; similarities between the data they generate, and possibly more importantly, their differences will help to constrain our models and ultimately enhance our understanding of brain function; they will define what aspect of brain function each technique probes and thus help to develop meaningful quantitative measures of activity. It might be thought that there would be little concordance between the hemodynamic response measured by BOLD fMRI and the neuromagnetic fields

---

\*Correspondence to: Claire M. Stevenson, Sir Peter Mansfield Magnetic Resonance Centre, School of Physics and Astronomy, University of Nottingham, University Park, Nottingham NG7 2RD. E-mail: claire.m.stevenson@nottingham.ac.uk

Received for publication 5 January 2009; Revised 23 December 2009; Accepted 24 December 2009

DOI: 10.1002/hbm.21016

Published online 16 April 2010 in Wiley Online Library (wileyonlinelibrary.com).

measured by MEG. But there are grounds for optimism: it has been suggested that the BOLD signal may be governed by local field potentials, which represent postsynaptic potentials or neuronal inputs rather than spiking output [Logothetis et al., 2001]. Postsynaptic potentials are also thought to be the basis of the neuronal signals measurable by MEG, and previous studies have shown a good correlation between fMRI BOLD data and time-locked, nonphase-locked oscillatory effects in MEG, strongly suggesting that the two processes are intimately linked [Brookes et al., 2005; Singh et al., 2002].

Simultaneous EEG/PET and especially EEG/fMRI, though challenging, have proved fruitful, enabling the hemodynamic response to be correlated directly with neural oscillatory activity in different frequency bands. The “default network,” first identified through the decreases in activity on task performance seen in PET and fMRI studies (see Buckner et al. [2008] for a review), is associated with a characteristic broad spectrum of frequency bands that covary with the BOLD fMRI signal on a timescale of 10–100 s. Together with electrocorticography (ECoG) measurements [Miller et al., 2009], these data lend weight to the neural (rather than vascular or artefactual) origin of the BOLD fluctuations, a topic that is still debated. Other “resting state networks” have their own characteristic frequencies: the sensorimotor resting network is primarily associated with a  $\beta$ -rhythm, whereas the visual resting network is associated with all classical rhythms apart from  $\gamma$  [Mantini et al., 2007]. Similarly, correlation methods have been used to identify the neuro-oscillatory changes that accompany the task-induced regional changes measured by PET in the sensorimotor and visual cortex [Oishi et al., 2007] and by fMRI in the sensorimotor cortex [Laufs et al., 2003; Parkes et al., 2006; Ritter et al., 2009]. Such studies provide strong evidence for the correlation between localized activity measured by PET or fMRI and patterns of neural activity. However, even with the use of ECoG, it is not possible to localize precisely the source of these oscillations. (The field pattern produced even by a small focal source extends, depending on its location and orientation, over an extended region, and usually will not be a maximum in the directly overlying electrode; indeed, if the orientation is unfavorable, such an electrode could fail completely to record the source. In the case of EEG, the field patterns are distorted further by the skull.) It is therefore important to establish, independently of the correlation evidence, that the measured neural oscillations originate from the activation foci identified by other neuroimaging techniques. For this, source rather than sensor space analysis is required. This is especially challenging for EEG though progress is being made (see, e.g., Brookes et al. [2009]), but is greatly improved in MEG where the magnetic, rather than the electric component of the electromagnetic field is measured, with the advantage that it passes through the skull undistorted. Although by no means perfect (the inverse problem has no unique solution), optimization, particularly of beamformer reconstruc-

tion methods [Robinson and Vrba, 1998], means that we can localize neuro-oscillatory activity with confidence [Brookes et al., 2008].

Recently, there has been much interest in  $\gamma$ -band activity determined by MEG and EEG [Hadjipapas et al., 2007; Hall et al., 2005; Joliot et al., 1994; Ribary et al., 1991; Swettenham et al., 2009], and task-related increases in  $\gamma$ -power, known as event-related synchronization (ERS), have been shown to be associated with brain activity as determined by fMRI BOLD [Lachaux et al., 2007]. In the visual system, the existence of a narrowband  $\gamma$ -rhythm is clear, but in other brain regions, specifically the sensorimotor system, it has been suggested that measured  $\gamma$ -ERS reflects a change in the broadband spectrum [Miller et al., 2007, 2009] that is more focal than the power changes in lower frequency rhythms, though this remains controversial. MEG studies have suggested that fluctuations in  $\alpha$ - and  $\beta$ -band activity are closely associated with BOLD signal change [Brookes et al., 2005; Singh et al., 2002], and concurrent EEG/fMRI studies have demonstrated a tight correspondence between the BOLD signal and task-related modulations of Rolandic  $\alpha$ - and  $\beta$ -rhythms [Laufs et al., 2003; Parkes et al., 2006; Ritter et al., 2009]. During simple motor activity, such as a cued fingertap, the  $\beta$ -band (15–30 Hz) rhythm exhibits a loss in power, event-related desynchronization (ERD) followed by a sharp increase (ERS) on movement cessation [Stancak and Pfurtscheller, 1995; Toma et al., 2000]. The loss in power during movement is consistent with the notion that  $\beta$ -band fluctuations represent cortical inhibition, which is released to enable activation. The power increase on movement cessation is commonly known as the post-movement  $\beta$ -rebound (PMBR) and, although its functional significance is not fully understood, it has been postulated that this rebound represents an uncoupling of the networks established during execution of the movement and a reinstatement of the idling  $\beta$ -rhythm [Pfurtscheller et al., 1996; Salmelin et al., 1995]. Given that the PMBR occurs after movement, another possibility is that the  $\beta$ -synchronization could reflect an active inhibition of the motor cortex by somatosensory afferents [Cassim et al., 2001]. A first aim of this study is, within the limits of accuracy of the MEG source localization and registration algorithms, to determine whether or not the MEG  $\beta$ -band response and the fMRI BOLD response to cued finger abduction are spatially congruent, or whether, as has been suggested [Miller et al., 2009], the former is more widely distributed. As a second more challenging test of the spatial congruity of MEG and fMRI BOLD responses, we use visual stimulation with a drifting sinusoidal grating, presented in one quadrant of the visual field. This is expected to elicit BOLD responses in distinct, noncontiguous regions of visual cortex, and MEG responses in discrete frequency bands ( $\alpha$ ,  $\beta$ , and  $\gamma$ ) and affords a good opportunity to establish which features (if any) collocate. We find it to be changes in  $\beta$ -band power, which best mimic the BOLD response.

Oscillatory activity and synchronization of oscillations in distinct frequency bands have been related to long-range

connectivity across the brain, particularly between cortical and subcortical areas in motor tasks [Schnitzler and Gross, 2005]. Indeed,  $\beta$ -oscillations are not restricted to primary motor areas, and  $\beta$ -ERD has been demonstrated in the lateral and inferior frontal lobes in association with a language task [Singh et al., 2002]. The oscillations are also present in deeper structures such as the thalamus [Paradiso et al., 2004] and striatum [Courtemanche et al., 2003], where, in agreement with recent work on oscillatory activity [Perez-Orive et al., 2002], it has been suggested that the  $\beta$ -band synchrony acts as a thresholding mechanism or localized gating of cortical activity. One idea is that  $\beta$ -band oscillations impose a certain level of synchronous activation, which must be overcome by the focal inputs before the target outputs can be affected. If indeed, it is the case that  $\beta$ -band oscillations act as a fundamental localized gating mechanism of cortical activity, then one might expect the characteristic modulations in  $\beta$ -band power, well known in the sensorimotor cortex, to be a more general phenomenon.  $\beta$ -band ERD has previously been observed in auditory cortex in association with speech comprehension and sensory gating [Eulitz and Obleser, 2007; Kisley and Cornwell, 2006] and in the occipital regions [Bauer et al., 2006], where it has been reported alongside an increase in power in the  $\gamma$ -band in response to a visual stimulus [Singh et al., 2002]. However, little has been reported on the amplitude of  $\beta$ -band effects and the stimulus dependency of these event-related modulations in power, particularly in the visual areas. A third aim of our study is therefore to establish whether the task-induced pattern of  $\beta$ -ERD/ERS that occurs in motor cortex is also present in visual cortex. We show that this is indeed the case by extracting “virtual sensor” traces from the foci of MEG power change identified in our drifting grating paradigm.

Unlike the situation for the simultaneous EEG/fMRI, or EEG/PET studies described earlier, our MEG and fMRI data are necessarily serially recorded (albeit using the same subjects and paradigms), and this restricts the possibilities for time series correlation studies, particularly those associated with spontaneous processes. However, it is still of great interest to ask how the MEG and fMRI responses are individually modulated by task duration and intensity and to compare them. The EEG/fMRI, PET correlation studies show a positive correlation for the default network, as would be expected if both are positive measures of activity. But in other resting state networks [Mantini et al., 2007] and in the Rolandic  $\beta$ -oscillations in the sensorimotor regions [Oishi et al., 2007; Ritter et al., 2009], the correlations are predominantly negative, that is, a decrease in neuro-oscillatory power is associated with an increase in activity (as measured by BOLD fMRI). This fits with the gating hypothesis described earlier. But what will happen as the stimulus is modulated? Certainly, we should expect that the ERD should be sustained as the stimulus duration increases, preserving a negative correlation with fMRI BOLD data, but what about variation with

stimulus intensity? If the ERD is a gating signal and the same area of cortex is being stimulated, then we should not necessarily expect an increase in ERD to accompany the increase in BOLD, and the correlation between them would be lost. The fourth and final aim of our study is to explore these possibilities by modulating the motor and visual paradigms in the following ways:

1. Cued finger abductions of varying durations.
2. Visual stimulation with a drifting, sinusoidal grating presented in one quadrant of the visual field at different contrast levels.
3. Visual stimulation with a drifting sinusoidal grating at fixed contrast but varying drift frequencies.

We show that  $\beta$ -ERD remains constant as the duration of motor activity or the grating contrast is varied, but that the level of  $\beta$ -band desynchronization increases with grating drift frequency.

## EXPERIMENTAL

All experiments were approved by the University of Nottingham Medical School Ethics Committee.

### Motor Study: Variation with Stimulus Duration

#### Subjects

Four healthy subjects (2 males and 2 females; age range, 21–24) took part in the study. All provided written, informed consent, had no neurological impairment, and classified themselves as right-handed.

#### Procedure

The motor paradigm comprised visually cued abductions of the right index finger (4 Hz). A trial contained a 2-s prestimulus rest period, finger movement of 1, 2, 4, or 6-s duration and a poststimulus rest period, which was varied to make each trial 12 s in total. For fMRI, trial durations were increased to 30 s to allow the hemodynamic response to return to baseline. The MEG experiment consisted of 30 trials per duration, whereas for the fMRI experiment 10 trials per duration were sufficient because of the higher signal to noise ratio [Brookes et al., 2005].

### Visual Contrast Response Experiment

#### Subjects

Eight healthy subjects (5 females and 3 males; age range, 22–29) participated in the contrast response study. A further three subjects (1 female and 2 males; age range, 24–29) took part in an extended study looking specifically at low contrasts. All gave written informed consent and had no neurological impairment.

## Procedure

The visual paradigm comprised a sinusoidal drifting grating, presented in a circular window with a visual angle of 5°. The grating was presented in the lower left hand quadrant of the visual field, shifted from a central marker by 3°. This minimized the possibility of magnetic field cancellation due to opposing dipoles on the cortical surface and the induction of correlated sources in the two visual hemispheres, which would pose a problem for beamformer analysis of the MEG data. The grating had a spatial frequency of three cycles per degree, and the drift rate was set to 8 Hz to produce maximal activation [Fox and Raichle, 1984]. Projectors were gamma corrected and five contrasts (0, 12.5, 25, 50, and 100% Michelson contrast) were presented pseudorandomly, with a medium gray background to avoid “after image” effects.

The extended low-contrast study used an identical visual stimulus with four Michelson contrasts, 3.1, 6.25, 12.5, and 100%, presented pseudorandomly.

For MEG, the initial contrast experiment comprised 30 trials per contrast, with the extended low-contrast study consisting of 40 trials per contrast. Because of the increased signal to noise in fMRI, for both experiments, 10 trials per contrast were used. Stimulus duration was 4 s, followed by a blank screen for 4 s in MEG and 16 s in fMRI.

## Visual Study: Drift Frequency Response

### Subjects

Six healthy subjects (3 females and 3 males; age range, 29–54) participated in the study. All gave written informed consent and had no neurological impairment.

### Procedure

The drift frequency paradigm used the same conditions as the contrast response experiment but with 100% Michelson contrast to produce maximal activation.

A preliminary experiment was undertaken using a static grating to check for effects of perceived motion in the grating, as might occur if one viewed a static grating following several drifting gratings. The stimulus timings and number of trials for the static stimulus were identical to those described earlier.

In the main experiment to assess response to motion, five drift rates (0, 2, 4, 6, and 8 Hz) were presented pseudorandomly, with a medium gray background. Stimulus duration was 4 s, followed by a blank screen for 4 s in MEG and 16 s in fMRI. Thirty trials per drift rate were acquired for MEG and 10 trials per drift rate for fMRI.

In the fMRI experiments, subjects viewed all visual stimuli, projected onto a screen at the end of the magnet bore, through a pair of prism glasses. In MEG, the stimulus was projected via a mirror system onto a screen inside the shielded room. For all visual experiments, subjects were

asked to fixate on a marker in the center of the screen for the duration of the experiment. To maintain attention, on cessation of the stimulus, subjects were asked to execute a button press to indicate the contrast or drift frequency of the stimulus. For all experiments, the same subjects were scanned in both MEG and fMRI.

## DATA ACQUISITION

MEG data were acquired using a 275-channel CTF Omega system (MISL, Port Coquitlam, Canada) in third-order synthetic gradiometer configuration, with a sample rate of 600 Hz and with a low-pass antialiasing filter with a cut-off of 150 Hz. A subject motion tolerance of 5 mm during the experiment was implemented, and trials containing excessive noise were excluded. (These bad trials usually comprised two or three of the 150 trials acquired in an experiment.) The d.c. offset was also removed on a trial by trial basis. Before data acquisition, digitization of the subject’s head shape was carried out using a 3D digitizer (Polhemus Isotrack). To coregister the MEG sensor locations to the subject’s brain anatomy, the digitized head shape was matched to a head surface extracted from an anatomical MR image using an in-house MATLAB script.

Anatomical MR images for coregistration with MEG data were acquired on a Philips 3T Achieva MR system, running a T1-weighted MPRAGE sequence with 1 mm isotropic resolution and a  $256 \times 256 \times 160$  matrix size. Imaging parameters were TR = 8.1 ms, TE = 3.7 ms, TI = 960 ms, shot interval = 3 s, flip angle = 8°, and SENSE factor 2.

BOLD-weighted functional MRI data were also acquired on the Philips 3T system using the following protocol. MR data consisting of 18 contiguous axial slices covering the motor or visual cortex, respectively, were acquired using a GE-EPI sequence (TR = 2,000 ms, TE = 45ms for the motor experiment, TE = 40 ms for the visual,  $3 \times 3 \times 3$  mm<sup>3</sup> voxels, 192 mm FOV). For the visual experiments, slices were centered on and oriented parallel to the calcarine fissure. For the motor experiments, slices were aligned parallel to the plane of the anterior and posterior commissures covering the motor regions. For both sets of experiments, the first four volumes were discarded to avoid spin saturation effects. Whole-head EPI images were also acquired for coregistration to anatomical images (TR = 10,000 ms, 50 slices,  $3 \times 3 \times 3$  mm<sup>3</sup> voxels).

## MEG DATA ANALYSIS

MEG data were analyzed using synthetic aperture magnetometry (SAM) [Robinson and Vrba, 1998]. Oscillatory activity in the 15–30 Hz band was examined, and spatial localization of both the characteristic  $\beta$ -ERD and poststimulus  $\beta$ -ERS was carried out using two sets of contrast windows for calculation of the SAM weights. Spatial localization of  $\beta$ -ERD (15–30 Hz) was achieved by comparison

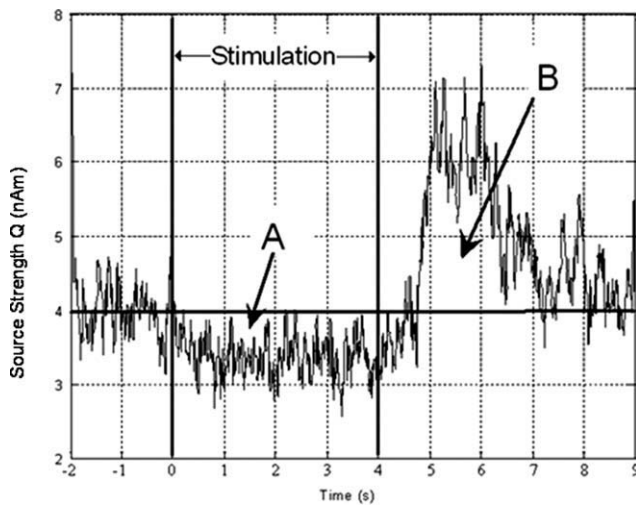


**Figure 1.**

Example time course of  $\beta$ -band activity taken from the motor experiment (4-s visually cued 4-Hz finger tap). Shown is the envelope amplitude of 15–30 Hz oscillatory activity taken from the peak of activity in the motor cortex. The response shown is averaged across four subjects. The characteristic ERD (Region A) followed by the postmovement rebound (Region B) can be clearly seen. Thick horizontal line shows the baseline for integration. Region A is the area integrated to assess linearity of the ERD. Region B shows the area integrated to assess linearity of the poststimulus ERS. Vertical solid lines show stimulus onset and cessation (at 2 and 6 s, respectively).

of oscillatory power in an active contrast window, spanning the stimulus presentation time (region A in Fig. 1) 2–6 s, and a passive time window spanning the pre or post-stimulus rest period. This passive window was set to 0–2 s in the motor study and 6.5–8 s in the visual study (i.e., when the poststimulus rebound had returned to baseline). An active window following stimulus cessation (region B in Fig. 1) at 6.5–8.5 s was used for poststimulus ERS localization with the passive windows maintained as before. Pseudo-*T*-stat images (1-mm<sup>3</sup> resolution) were created showing regions of oscillatory power change within the  $\beta$ -band. The same SAM analysis was also carried out in the  $\gamma$  (60–80 Hz) and  $\alpha$  (8–13 Hz) bands.

Using the beamformer weights derived in computation of the SAM image, it is possible to compute a spatially selective reconstruction of the time course of neuronal activity, known as a virtual sensor. Virtual sensor traces were extracted from peaks of activity in the SAM images, and time courses of electrical oscillatory power were obtained by applying a Hilbert transform to the virtual sensor data to obtain the analytic signal. The absolute value of the analytic signal was then averaged across trials to yield the envelope of oscillatory power in the  $\beta$ -band [Blackledge, 2003]. Linearity of the  $\beta$ -response was assessed by the integration of the analytic signal. The base-

line for integration was taken to be a mean of the data in the passive window. The same time windows used to create images of  $\beta$ -ERD and  $\beta$ -rebound were used as the limits of integration. Areas calculated were mean corrected and averaged across subjects before plotting the respective linearity curves.

## fMRI DATA ANALYSIS

Preprocessing of fMRI data was carried out using both in-house Matlab programs and SPM5. Motion correction

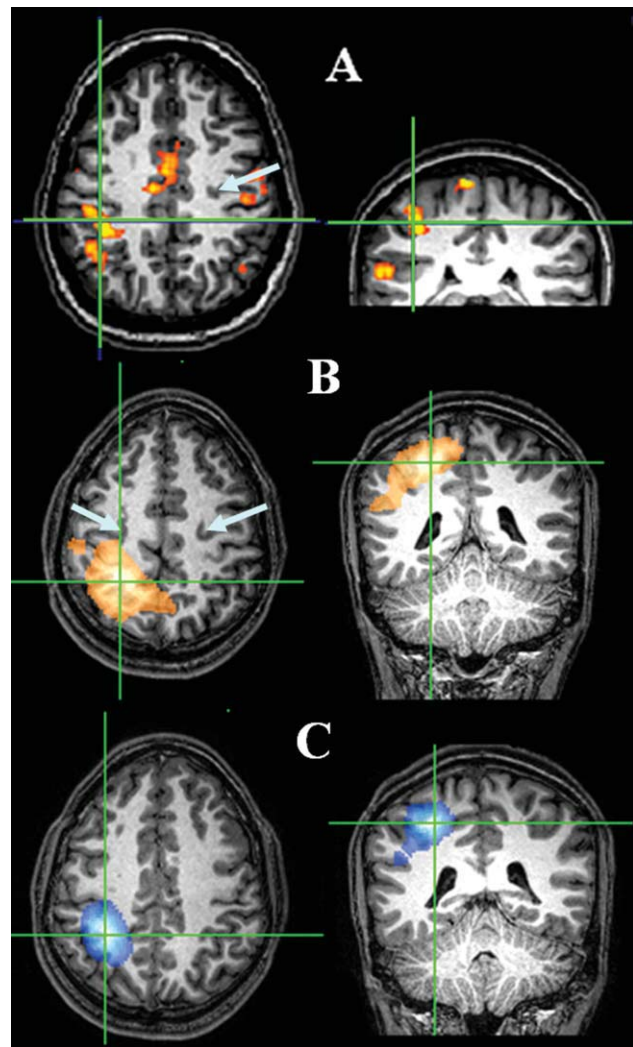


**Figure 2.**

Functional localization of motor activity using both MEG and BOLD. Spatial localization of MEG and BOLD for a single representative subject for the finger tap experiment. Cross hairs show maxima in responses and arrows depict central sulcus location. (A) BOLD  $P < 0.05$  corrected, (B)  $\beta$ -ERS  $T > -1.2$ , and (C)  $\beta$ -ERD  $T < 1.2$ .

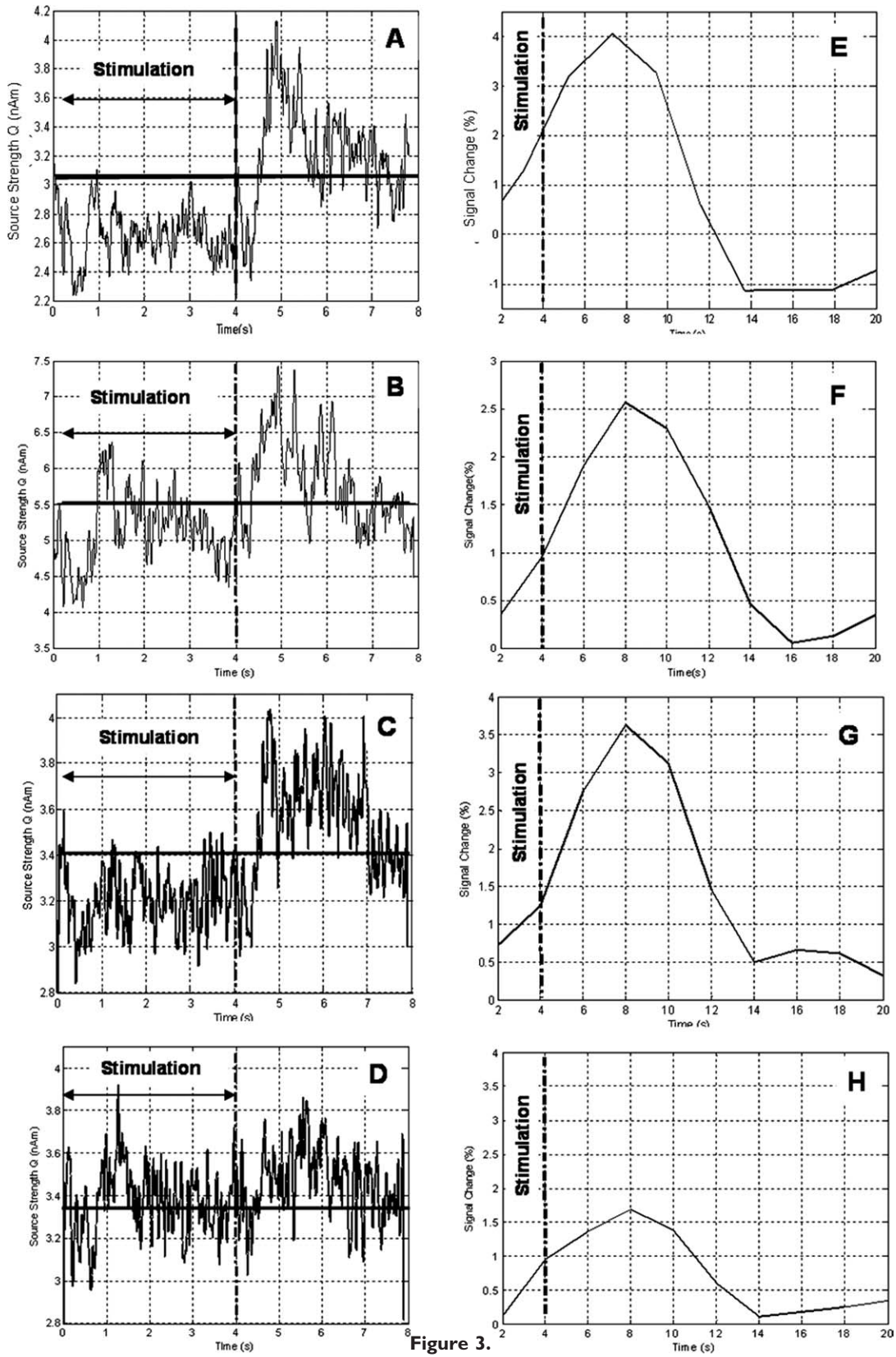


Figure 3.

was carried out in SPM5: images were registered to the first volume acquired, and motion correction parameters were saved for later inclusion in the design matrix. Low-frequency drift was removed using a polynomial linear regression technique programmed in Matlab. Data were spatially smoothed using a 5 mm Gaussian kernel in SPM5.

Areas of significant ( $P < 0.05$  corrected) BOLD contrast were identified using the SPM5 general linear model. A box car design matrix was created, with timings for onsets of each contrast being taken from the stimulus presentation log files and motion parameters included to account for subject movements. The box-car function was convolved with the standard canonical HRF in SPM5 [Friston et al., 1998] to account for hemodynamic effects.

For spatial comparison with MEG results, the statistical parametric maps were coregistered to each subject's anatomical image. To do this, brain extraction was applied to the 1 mm isotropic anatomical image using BET [Smith, 2002] and a whole head EPI, collected directly after functional data acquisition, was coregistered to the extracted brain. Image volumes acquired during the experiment were coregistered to the registered whole head EPI and the same transform applied to the statistical parametric map.

Coregistered functional images were overlaid onto the anatomical image and voxel coordinates of the global maximum noted. For the visual experiments, where there were multiple peaks of significant activity, the voxel coordinates of the global maximum, and the maximum of the second most significant cluster in the visual cortex were noted (threshold  $P < 0.05$  corrected and extent five voxels). Cluster level analysis was carried out in SPM5.

Data were taken from a  $9 \times 9 \times 9$  mm<sup>3</sup> cubic region centered on the global maximum and used to obtain average time-courses of the hemodynamic response. Linearity of the BOLD response was assessed by integration of the BOLD time-course over the entire trial length. Baseline for integration was taken to be the mean value of the data acquired during the time period where there was no finger movement or equivalently no visual stimulus present on the screen (i.e. zero contrast in the visual experiments). Calculated areas were mean corrected and averaged across subjects before plotting the respective linearity curves.

## SPATIAL COMPARISON

To make a quantitative spatial comparison between MEG and BOLD data, the locations of the maxima of each response were recorded. Where there were multiple peaks in the SAM images, as was the case for  $\beta$ -band oscillatory activity, the voxel co-ordinates of the two peaks with largest pseudo- $T$ -statistic were noted. The voxel co-ordinates of the two most significant BOLD peaks were also recorded, and the Euclidean distances between MEG peaks and BOLD peaks were computed.

## RESULTS

### Spatiotemporal Signature of Responses

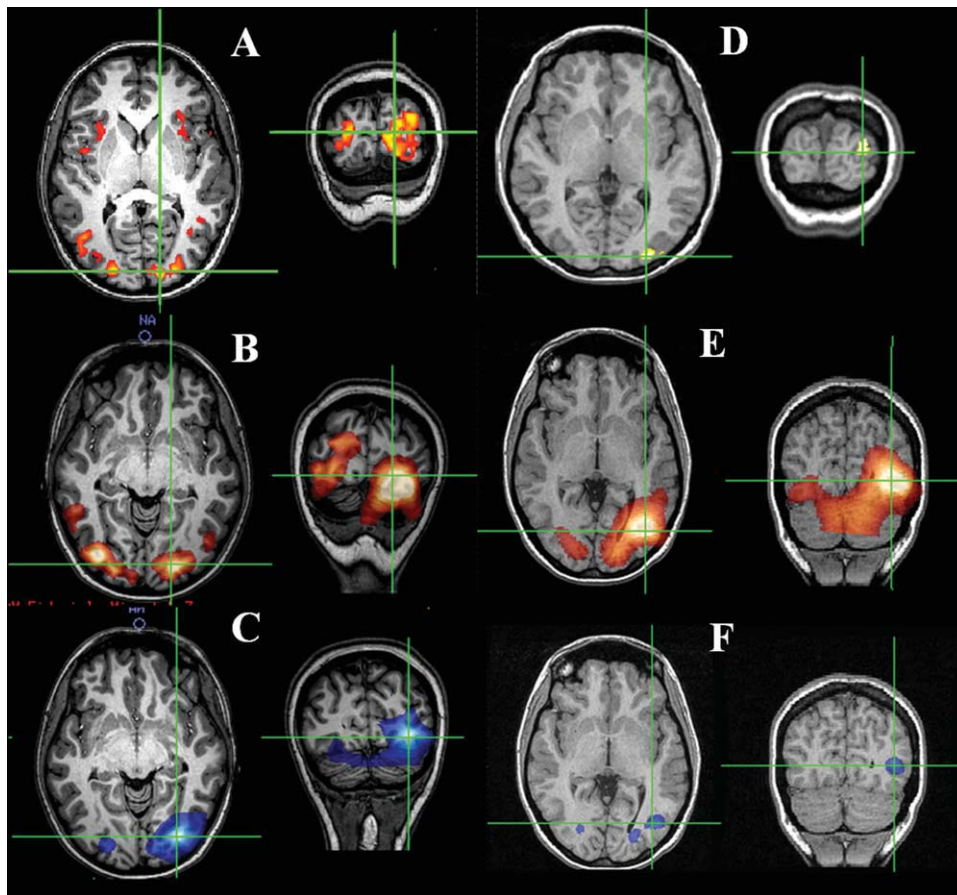
#### Motor study

Figure 1 shows the temporal signature of the envelope of  $\beta$ -band oscillatory activity in the contralateral motor cortex. The expected event-related desynchronization and postmovement rebound of power in the  $\beta$ -band are demonstrated. Figure 2A–C illustrates the spatial colocalization of the  $\beta$ -ERD, ERS, and BOLD data. The BOLD functional image (Fig. 2A) contains a peak of activity in the contralateral primary motor cortex, together with contributions from ipsilateral motor cortex, supplementary motor area, and sensory areas. The loss in  $\beta$ -power (Fig. 2C) localizes to the contralateral primary motor cortex, as has previously been seen both in MEG and EEG [Jurkiewicz et al., 2006]. Similarly distributed MEG activity occurs ipsilaterally as seen on lowering the statistical threshold. However, due to its low pseudo- $T$ -stat, we did not subject the ipsilateral activity to further analysis. The rebound  $\beta$ -activity (Fig. 2B) appears shifted from the ERD location and exhibits a more broadly distributed response covering contralateral premotor, motor, and sensory cortex. The mean 3D displacement in the peaks of the ERD and ERS was found to be  $2.9 \pm 0.9$  cm. However, despite all subjects in the motor study showing a difference in peak locations for  $\beta$ -ERD and ERS there appears to be no common direction in the displacement across the four subjects, and it is therefore unclear whether this represents a true spatial

**Figure 3.**

Correspondence of MEG and BOLD in central and lateral visual areas for drifting and static gratings. **A:** Envelope of oscillatory power in  $\beta$ -band at peak of activity in the central visual areas contralateral to stimulus presentation for a drifting grating (8 Hz). **B:** The corresponding MEG time course for a static grating (taken from the same location as the trace in A). **C:** Envelope of oscillatory power in  $\beta$ -band at peak of activity in the lateral visual areas contralateral to stimulus presentation for a drifting grating (8 Hz). **D:** The corresponding MEG time course for a static grating (taken from the same location as the trace in A). **E:** Average BOLD time course extracted from the SPM region of ac-

tivity ( $P < 0.05$  corrected extent five voxels) in the central visual areas for a drifting grating (8 Hz). **F:** The corresponding BOLD time course from central visual areas for the static grating. **G:** Average BOLD time course from the lateral visual areas for a drifting grating (8 Hz). **H:** The corresponding BOLD time course from lateral visual areas for the static grating. In all plots, stimulus onset is 0 s and the vertical dashed line at 4 s indicates stimulus cessation. The solid horizontal line in the MEG time-courses on the left indicates the baseline activity. The reader should note the difference in timescales for the MEG and BOLD time courses due to the protracted haemodynamic response.



**Figure 4.**

Spatial localization for visual experiments. Cross hairs show maxima in responses [8 Hz drift frequency, 100% Michelson (A) BOLD  $P < 0.05$  corrected, (B)  $\beta$ -ERS  $T > 1.2$ , (C)  $\beta$ -ERD  $T > 1.2$ ], [static grating (D) BOLD  $P < 0.05$  corrected, (E)  $\beta$ -ERS  $T > 1.2$ , and (F)  $\beta$ -ERD  $T > 1.2$ ].

separation in the neural effects or is simply an artefact of the source localization technique.

An evoked response was also seen at the peak location of the  $\beta$ -ERD; however, no robust time locked nonphase locked activity in other frequency bands was observed in any subject. For the purposes of this study, data analysis was therefore limited to time-locked oscillatory activity in the  $\beta$ -band.

### Visual study

Figure 3A,C shows the envelope of oscillatory activity in the  $\beta$ -band at the peak of activity in the contralateral central visual areas (A) and in the lateral visual area (MT) (C) for a grating drift frequency of 8 Hz. The modulation in activity both during and poststimulation can be seen clearly and is very similar to that observed in the motor study. There is a loss in power at stimulus onset ( $t = 0$  s), which is sustained during the 4 s of stim-

ulation and continues for  $\sim 0.5$  s after stimulus cessation. This is then followed by a rebound in activity, with a power increase above baseline for  $\sim 2$  s. The oscillatory activity then returns to baseline. Figure 3B,D shows equivalent time-courses from the same locations (contralateral central visual areas and MT) on presentation of a static grating. It can be seen that the magnitude of the modulation in MT is significantly reduced: the ERD represents an average local loss in power in the 15–30 Hz band of  $1\% \pm 1\%$  in comparison with  $6\% \pm 2\%$  for a grating with a drift rate of 8 Hz, and the ERS represents an average local increase in power in the 15–30 Hz band of  $7\% \pm 3\%$  in comparison with  $11\% \pm 3\%$  for the drifting grating. The corresponding BOLD time-courses are shown in Figure 3E–H. These agree with the  $\beta$ -band data in that the amplitude of the BOLD response in MT due to a static grating is less than half that elicited in the same location by a grating with a drift frequency of 8 Hz.



**TABLE I. A spatial comparison of fMRI and MEG effects for each of the subjects in the visual contrast experiment**

Subject	Global max contralateral peak location (voxel coordinates)	Euclidean distance (mm)	Second most significant peak ipsilateral location (voxel coordinates)	Euclidean distance (mm)
1. fMRI	142, 211, 138		113, 209, 138	
MEG $\beta$ -ERD/S	146, 208, 136	5.39	117, 208, 132	7.28
MEG $\gamma$ -ERS	137, 202, 132	11.90	N/A	N/A
2. fMRI	145, 221, 115		119, 230, 127	
MEG $\beta$ -ERD/S	143, 219, 113	3.46	114, 224, 123	8.78
MEG $\gamma$ -ERS	139, 206, 107	18.00	N/A	N/A
3. fMRI	142, 214, 105		115, 214, 103	
MEG $\beta$ -ERD/S	138, 218, 103	6.00	103, 213, 101	12.2
MEG $\gamma$ -ERS	134, 206, 105	11.30	N/A	N/A
4. fMRI	146, 199, 102		116, 193, 104	
MEG $\beta$ -ERD/S	148, 205, 120	19.10	93, 197, 119	27.7
MEG $\gamma$ -ERS	134, 203, 110	15.00	N/A	N/A
5. fMRI	153, 217, 88		110, 217, 94	
MEG $\beta$ -ERD/S	153, 217, 102	14.00	108, 217, 110	16.1
MEG $\gamma$ -ERS	143, 217, 110	17.00	N/A	N/A
6. fMRI	130, 217, 151		119, 214, 162	
MEG $\beta$ -ERD/S	137, 215, 150	7.35	114, 227, 162	13.9
MEG $\gamma$ -ERS	148, 214, 156	18.90	N/A	N/A
7. fMRI	149, 206, 128		104, 218, 128	
MEG $\beta$ -ERD/S	153, 216, 121	12.80	98, 211, 127	9.27
MEG $\gamma$ -ERS	N/A	N/A	N/A	N/A
8. fMRI	147, 210, 120		108, 210, 120	
MEG $\beta$ -ERD/S	143, 212, 124	6.00	100, 203, 114	12.2
MEG $\gamma$ -ERS	139, 210, 121	8.06	N/A	N/A
Mean peak displacement (mm)				
fMRI vs. $\beta$ -ERD		$9 \pm 2$		$13 \pm 2$
fMRI vs. $\gamma$ -ERS		$14 \pm 2$		No response

Data shown are for 100% Michelson Contrast with a drift rate of 8 Hz. Voxel co-ordinates of the global maximum and the second most significant cluster (extent: five voxels, threshold  $P < 0.05$ ) in the BOLD statistical parametric map are compared to voxel co-ordinates of the two peaks with the largest pseudo- $T$ -stat in the SAM images of  $\beta$ -band activity (15–30 Hz). In addition, the peak in  $\gamma$ -band activity (60–80 Hz) is compared to the global maximum of BOLD activity. The Euclidean distance between peak locations in the respective modalities is computed.

Figure 4A shows the locations of visual BOLD responses to a drifting grating (100% Michelson contrast and drift frequency 8 Hz) presented in one quadrant of the visual field. The global maximum is found in the contralateral primary visual cortex, with activity of lower threshold in the ipsilateral primary visual cortex. Activity also appears bilaterally in the more lateral visual regions such as MT, which is consistent with previous studies [Tootell et al., 1995] and can be attributed to the drifting of the grating. The spatial distribution of BOLD activity is echoed in both the  $\beta$ -ERD and the poststimulus  $\beta$ -ERS as shown in Figure 4B,C. This is consistent with a previous MEG study [Fawcett et al., 2004], which, using a counter-phasing rather than a drifting stimulus, demonstrated predominantly  $\beta$ -ERD in V5/MT. Unlike the motor response, the location of the rebound seems to overlie that of the  $\beta$ -ERD.

The spatial localization of the activity elicited by a static grating is shown in Figure 4D,E. Strong activation in contralateral primary visual cortex is seen in the BOLD

response, but activity in MT though still present, appears at a lower  $T$ -statistic (Fig. 4D), consistent with the known role of area MT for encoding motion information. This is also reflected in the  $\beta$ -band ERS (Fig. 4E) and in the  $\beta$ -band ERD (Fig. 4F).

Previously, focal induced gamma (60–80 Hz) ERS has been found to be highly spatially coincident with the BOLD response [Brookes et al., 2005]. In our visual studies,  $\gamma$  (60–80 Hz) oscillatory activity was observed in seven of eight subjects and showed a single peak of significant activity. The remaining subject showed no significant activity within this frequency band. Despite a concomitant increase in gamma power at the global maximum of the BOLD response in contralateral central visual areas, we did not observe ipsilateral  $\gamma$ -activity in the primary visual areas nor did we observe  $\gamma$ -activity in the lateral visual areas.

Table I shows a comparison of the peak locations in MEG (both  $\beta$ -band activity and  $\gamma$ -activity) and peak locations in BOLD fMRI for all subjects in the visual contrast experiment. The functional images were registered to 1-mm isotropic

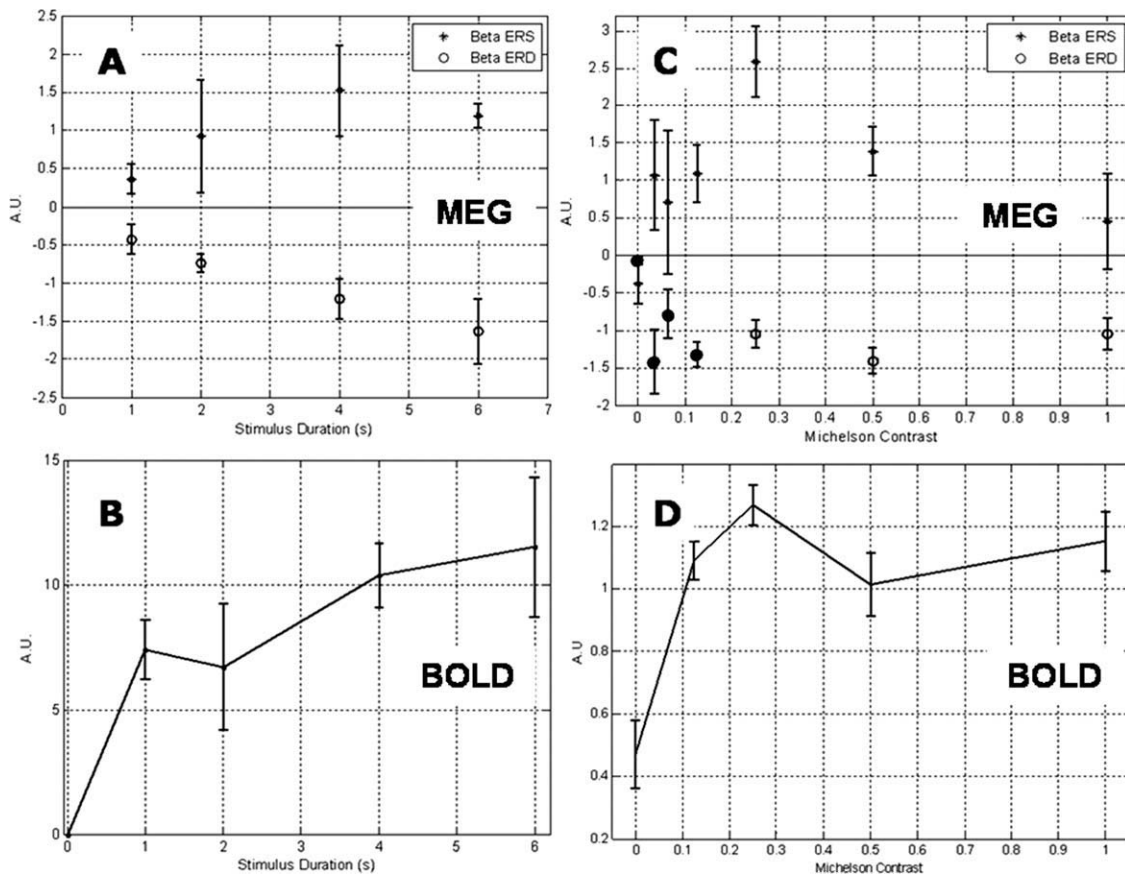


Figure 5.

Modulation of  $\beta$ -band and BOLD activity with respect to stimulus amplitude and duration. Plots (A–D) show the modulation of MEG and BOLD responses on manipulation of stimulus duration and amplitude. All plots are mean corrected, averaged across subjects, and error bars represent standard error across subjects. A: Total amount of  $\beta$ -ERD (○) and  $\beta$ -rebound (+) in the contralateral primary motor cortex for finger movement of various durations, assessed by integration of the absolute value of the analytic signal. Note the linear increase in  $\beta$ -ERD as stimulus duration increases. B: Corresponding BOLD data for the

motor experiment. Plotted are the areas under the respective BOLD time courses, taken from a  $9 \times 9 \times 9 \text{ mm}^3$  volume around the global maximum. The area under each of the BOLD curves is plotted with respect to stimulus duration. C: Total amount of  $\beta$ -ERD (○) and ● (low-contrast experiment) and  $\beta$ -rebound (+) in contralateral primary visual cortex, assessed by integration of the absolute value of the analytic signal, for gratings of various contrast. D: BOLD derived contrast response curve for central visual areas contralateral to stimulus presentation.

anatomical images, and so the units of the voxel coordinates can be taken to be millimeters. A good spatial correlation is observed between the single  $\gamma$ -peak and the BOLD response in contralateral primary visual cortex. There is even better agreement between the response in the MEG  $\beta$ -band and the BOLD data. The global maximum in  $\beta$ -activity is displaced from the global maximum of the BOLD response by a mean distance of  $9 \pm 2 \text{ mm}$  in comparison with  $14 \pm 2 \text{ mm}$  for the peak of  $\gamma$ -activity. What is even more compelling is the coincidence between the regions of secondary  $\beta$ -peaks and the BOLD data. This seems to be unique to the  $\beta$ -band in the experiments reported here.

### Linearity of Response

#### Motor study: duration

Figure 5A,B shows the linearity of the responses with respect to the duration of the finger tap experiment. Figure 5A shows a roughly linear increase in the integrated  $\beta$ -power loss (○) with respect to stimulus duration (i.e. the  $\beta$ -power loss is constant over the stimulus interval). The integrated rebound response (Fig. 5A (+)) increases with stimulus duration up to about 4 s. In contrast, the BOLD response, shown in Figure 5B, is characterized by a large

response to a short duration stimulus, increasing slowly as the duration is increased.

### Visual study: variation with contrast

The linearity results of the contrast response experiment are shown in Figure 5C,D. The variation of  $\beta$ -ERD is shown in Figure 5C (○), and it is clear that it is not modulated by stimulus contrast. The results from the separate low-contrast experiment are included in Figure 5C (●), and it can be seen that, despite being acquired in different subjects on a separate occasion, they agree well with the other contrast response data. Furthermore, these results show no stimulus dependency of the amplitude of  $\beta$ -ERD even at very low contrast.

$\beta$ -band ERD thus appears to have a distinct ON/OFF property. In terms of a fractional signal change in  $\beta$ -power during stimulation, this corresponds to a  $12\% \pm 3\%$  loss in  $\beta$ -power (averaged across subjects and contrasts).

Just as for the motor study, a strong rebound in  $\beta$ -band activity ( $\beta$ -ERS) is observed on cessation of the visual stimulus (Fig. 3A,B). The integrated response is shown in Figure 5C where it is clear that it increases with contrast at low contrasts ( $\leq 0.25$ ), thereafter declining. The largest rebound response (seen at 25% contrast) represents a  $15\% \pm 3\%$  increase in  $\beta$ -power.

The BOLD-derived contrast response curve exhibits a non-linear trend but as for the motor study, a significant response is elicited even by a low stimulus (contrast), which increases more slowly as the contrast is increased.

### Visual study: variation with drift frequency

Figure 6 depicts the variation in  $\beta$ -band activity in area MT elicited on presentation of a grating with a range of drift frequencies. Unlike the results previously obtained in the visual contrast experiment and the motor duration task, Figure 6A shows an increase in the magnitude of the  $\beta$ -ERD (○) as the drift rate of the stimulus increases. The  $\beta$ -rebound (+) displays a less distinct trend and there seems to be little variation in its magnitude with stimulus drift frequency.

Figure 6B illustrates the BOLD drift frequency response in contralateral MT. It is clear that the BOLD signal is also modulated by drift frequency in a similar (but inverse) fashion to the  $\beta$ -ERD. There appears to be a degree of saturation at higher drift frequencies.

## DISCUSSION

### Spatiotemporal Signature of Responses

Previous studies have demonstrated a good spatial correlation between BOLD fMRI data and time-locked, non-phase locked oscillatory effects in MEG, particularly in the  $\gamma$ -band, strongly suggesting that the two processes are intimately linked [Brookes et al., 2005; Singh et al., 2002]. In this work, we have shown that there is also excellent spa-

tial colocalization of BOLD responses and  $\beta$ -band effects, adding further weight to these previous arguments.

### Motor experiment

The expected correlation between BOLD and MEG is demonstrated in the spatial colocalization of the  $\beta$ -ERD and ERS in the motor experiment and the corresponding BOLD data. Given that no prior information was used in the localization of either of the effects, this is impressive, particularly as MEG and fMRI measure fundamentally different phenomena. Neuronal desynchronization is thought to be due to asynchronous firing within cortical networks and hence an indicator of neural activation in sensorimotor cortex. The  $\beta$ -ERD peak in the contralateral primary motor cortex is consistent with this notion and is found in the region that is known to be active during simple finger movement. The fact that a similar  $\beta$ -desynchronization of lower pseudo- $T$ -stat is found in the same part of the ipsilateral sensorimotor cortex (results not shown) would suggest that this region of cortex is also involved to some degree in unilateral finger movement. This is also demonstrated in the BOLD data, and previous MEG studies have found evidence of the involvement of the ipsilateral cortex in execution of unilateral finger movement [Cheyne et al., 2006; Taniguchi et al., 2000]. The  $\beta$ -rebound is found displaced from the ERD, in agreement with some previous motor studies using MEG [Jurkiewicz et al., 2006] and may suggest a slightly different role of the ERS to the ERD. However, the ERS is somewhat less consistent than the ERD in its spatial localization, and so it is not possible to draw firm conclusions.

### Visual contrast experiment

$\beta$ -activity in the visual cortex is less well documented. We find that the characteristic loss in power during stimulation followed by a rebound poststimulus, lasting  $\sim 1.5$ – $2$  s, which has been thoroughly described for motor experiments, is also evident in the visual system. This reinforces the idea that the ERD/ERS phenomena in the  $\beta$ -band are general in nature and not specific to sensorimotor cortex.

The spatial colocalization of the  $\beta$ -ERD/ERS and the BOLD response in the visual cortex is compelling. We find both BOLD and  $\beta$ -ERD responses in the central and lateral visual areas and the excellent spatial colocalization of the MEG derived  $\beta$ -band oscillatory activity and the BOLD response would suggest that the two processes are intimately related. Microelectrode work in macaques has demonstrated highly localized pockets of reduced synchrony in striatal  $\beta$ -band oscillations on execution of an oculomotor saccade task. The focal nature of the losses in  $\beta$ -power seen here may intimate that the oscillations are replicating in the cortex the behavior that has previously been seen in the deep structures such as thalamus and striatum [Courtemanche et al., 2003].

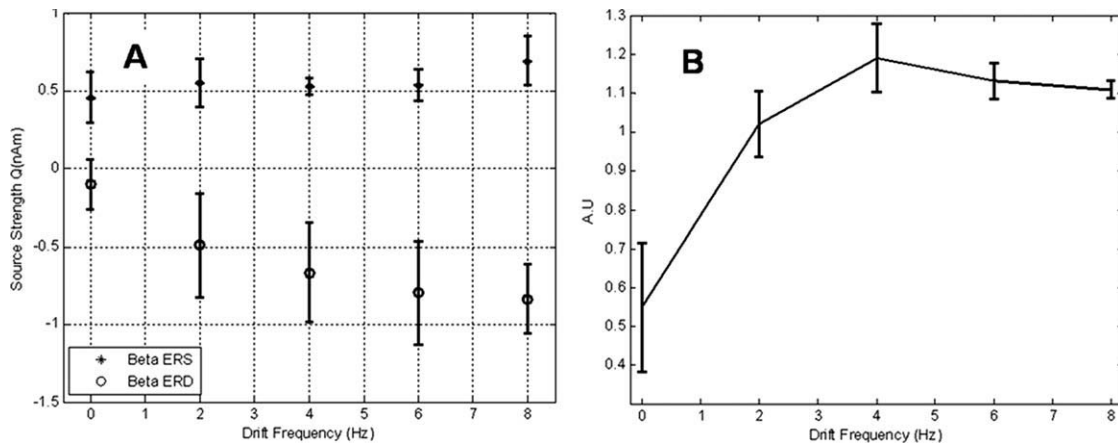


Figure 6.

Modulation of MEG and BOLD in lateral visual areas due to variations in stimulus drift frequency. Plots (A) and (B) show the modulation of MEG and BOLD responses on manipulation of stimulus drift frequency. All plots are mean corrected, averaged across subjects, and error bars represent standard error across subjects. A: Total amount of  $\beta$ -ERD (○) and  $\beta$ -rebound (+) in lateral visual

areas, contralateral to stimulus presentation. Modulation of  $\beta$ -activity due to stimuli of various drift frequencies was assessed by integration of the absolute value of the analytic signal. B: Corresponding BOLD data for the drift frequency experiment. Plotted are the areas under the respective BOLD time courses, taken from a  $9 \times 9 \times 9 \text{ mm}^3$  volume around the global maximum.

The spatial colocalization of  $\beta$ -band activity and BOLD is highlighted in Table I. The Euclidean distances between MEG and BOLD peaks are similar to those previously reported: 10.3–28.7 mm for MEG oscillatory activity across a range of frequencies [Winterer et al., 2007], and 6.46 mm [Muthukumaraswamy and Singh, 2008] and  $9 \pm 15$  mm [Brookes et al., 2005] between  $\gamma$ -band oscillatory activity and BOLD. It has been demonstrated in a retinotopic mapping MEG experiment that the spatial resolution in the visual cortex varies between 2 and 20 mm [Barnes et al., 2004]. Differences in locations of MEG and BOLD peaks may be attributed in part to errors during coregistration of both sets of functional data to anatomical images. Although some error will arise due to the registration of functional to anatomical MR data, the largest contributor to this type of error is coregistration of MEG data: the commonly used procedure of matching fiducial markers and digitized surface matching is prone to errors due to misplacement of fiducial markers and distortion in MR images arising from susceptibility artefacts. It is well known that geometric distortion in the MR image due to magnetic susceptibility variations is greatest at air/tissue interfaces, in regions such as the mouth, nasal sinuses, and ears, where fiducial markers are likely to be placed [Park et al., 1988]. It has been shown that displacement of the fiducial marker in the nasion region by 1 mm may produce errors of several millimeters or even centimeters in the posterior visual cortex due to a leveraging effect [Singh et al., 1997]. It should also be noted that (as in this case) functional data sets for BOLD have often been interpolated from an acquisition voxel size of typically  $3 \times 3 \times 3 \text{ mm}^3$  and overlaid onto a 1-mm isotropic anatomical image. Hence a discrepancy of 9 mm between

the maximum  $\beta$ -peak and the global maximum of the BOLD response is actually only equivalent to the Euclidean distance across two functional voxels. There is also an error that can be attributed to source localization in MEG; however, this is difficult to assess as simulations have shown that spatial resolution of the volumetric beamformer images is inhomogeneous across the brain and varies according to source strength [Barnes and Hillebrand, 2003].

Of particular interest here is the agreement between BOLD and  $\beta$ -band activity where multiple peaks in both data sets are found in the same location. This is in contrast to  $\gamma$ -activity, which despite a good spatial agreement with the global maximum of the fMRI BOLD response showed no further significant peaks in any subject. This is consistent with work by Miller et al. [2007], where ECoG data in the motor cortex showed a more widespread response in lower frequency bands such as  $\beta$  in comparison with a focal response in broadband high frequencies (similar to our  $\gamma$ -response).

The difference in spatial localization of peaks of induced  $\gamma$  and  $\beta$ -activity is interesting and suggests different functional roles for the two oscillatory rhythms. It has been shown that  $\gamma$ -oscillations develop due to low-level stimulus properties such as luminance contrast [Henrie and Shapely, 2005] and contour [Gail et al., 2000], whereas  $\beta$ -activity has been linked to visual attention [Wrobel, 2000] and a measure of cortical excitability, rather than playing an active role in processing or encoding visual information. However, these differences are within the inherent spatial resolution of the two techniques, and therefore their detailed interpretation would be largely speculative.

Although it is clear from many studies that gamma plays an important role in the encoding of neural

information, the results from this set of experiments highlight the differing roles of  $\gamma$  and  $\beta$ -oscillatory activity, and this should be taken into account when considering their possible contributions to the BOLD response.

As for the motor study, the small differences in location of the  $\beta$ -ERS and ERD in the visual cortex may reflect the difference in signal to noise of the two responses rather than a spatial separation between them. This is reinforced by the inconsistency observed in their relative locations. Should it prove possible to separate sufficiently the  $\beta$ -ERD and ERS in time, it may be possible to use the greater spatial accuracy of fMRI to provide a definitive answer. Future studies will explore this possibility.

### Linearity of Responses

#### Motor: duration study

The amplitude of  $\beta$ -band desynchronization is constant during the motor activity, with no evidence of any significant degree of adaptation. This is evident in the integral of power loss, which increases approximately linearly with stimulus duration (Fig. 5A). This might be expected if  $\beta$ -activity is an idling rhythm, which is 'switched off' during cortical activity, that is, it operates as a gate for cortical activation. Interestingly, the desynchronization does not revert back to baseline directly on stimulus cessation. Instead, there is a continued desynchronization for  $\sim 0.5$  s following the end of the stimulus and it then returns to baseline via the  $\beta$ -ERS. This may correspond to the re-engagement of thalamocortical inhibitory circuits that were disengaged during stimulation. If this is the case, it is unclear why the magnitude of the postmovement ERS should increase with stimulus duration (Fig. 5A). It may be that the longer the cortical network is disengaged, the more energy is required to reinstate them.

The magnitude of the BOLD response does not increase linearly with stimulus duration in the motor cortex (Fig. 5B), and this is in agreement with previous studies [Glover et al., 1999]. Rather there is a large response to a short period of motor activity followed by a slower increase with duration at longer times. The apparent discrepancy in the  $\beta$ -ERD response to increasing stimulus duration and that of the BOLD response is likely to be the result of many factors. It is highly improbable that  $\beta$ -desynchronization alone is driving the BOLD response. The neuromagnetic signals measured by MEG are rich and modulation of  $\beta$ -band oscillatory activity is just one example of event-related neuromagnetic phenomena. Furthermore, unlike MEG, BOLD does not provide a direct measure of neural activity, and the response itself is governed by a number of factors including: changes in CBF, CBV, blood oxygen extraction, and local metabolism driven by neural activity. Despite maintaining a close relationship in terms of spatial colocalization of the two effects, the results here show a divergence in task-related amplitude modulation of the Rolandic rhythms and the BOLD response. This is of particular interest as it differs somewhat from results

derived from resting state data [Laufs et al., 2003; Parkes et al., 2006; Ritter et al., 2009] where close negative correlations have been demonstrated between spontaneous fluctuations in amplitude of the Rolandic rhythms and BOLD. Here, the negative correlation is preserved, with a loss in  $\beta$ -power relating to an increase in BOLD amplitude, but stimulus specific modulations in amplitude in the two effects do not vary in the same manner. However, the discrepancy is entirely consistent with a gating role: the gate is either open or closed, but the cortical activity that follows is subject to many controlling factors, including attention.

#### Visual study: variation with contrast

The response of the  $\beta$ -oscillatory activity to stimulus contrast (Fig. 5C) agrees very well with the characteristics of the response seen in the motor experiment. It is clear that the magnitude of the ERD is not modulated by stimulus contrast. This would support the argument that  $\beta$ -oscillations have gating properties and that the gate is either open or closed. The ERS is again nonlinear, first increasing with contrast, and then declining at higher contrasts. Similarly, the BOLD-derived contrast response curve (Fig. 5D) is nonlinear and appears to saturate at higher contrasts. This is characteristic of contrast response measured in central visual areas using BOLD fMRI [Tootell et al., 1995]. Even at low contrast, the  $\beta$ -band ERD is not modulated by contrast and appears to have a distinct ON/OFF property. It seems that  $\beta$ -band oscillatory activity may perform a similar role in the visual cortex to that in the sensorimotor cortex where it has been well studied.

The lack of contrast dependency in the  $\beta$ -band response could also be explained if  $\beta$ -power change is reflecting activity from cells which saturate at very low contrasts. This would intimate that at sufficiently low contrasts, there may be some modulation. Although contrast response of  $\beta$ -activity in lateral visual areas was not examined as part of this study it proves an interesting point for future study as it is thought that the predominant input to MT is a magnocellular projection from layer 4B of V1 [Born and Bradley, 2005]. It has previously been demonstrated that magnocellular neurons have a lower contrast threshold and saturate at much lower contrasts than their parvocellular counterparts [Allison et al., 2000; Derrington and Lennie, 1984]. This would therefore provide an opportunity to compare the  $\beta$ -contrast response in areas with known differences in saturation levels.

#### Visual study: variation with drift frequency

The tight spatial correspondence between the  $\beta$ -band activity and BOLD is also seen in the results for the drift frequency experiment both in the central visual cortex and in the lateral visual areas. Although  $\gamma$ -band activity was observed in the central areas, there was no significant activity in other frequency bands present in the lateral visual

areas and the modulation of activity here was unique to the  $\beta$ -band.

It is not entirely clear how the response of the  $\beta$ -band activity to increasing drift frequency fits with the notion of a gating property of  $\beta$ -oscillations. However, one would postulate that this reflects the gating of an increased area of cortex on a microscopic rather than a macroscopic scale. The increase in BOLD response with drift frequency supports this idea. Previous fMRI literature has also shown an increase in BOLD response with drift frequency in V5/MT, with a typical tuning curve being nonlinear and taking the form of an “inverted U.” However, the velocity of stimulation reported to induce the maximum BOLD response is variable, ranging from 4.5°/s [Singh et al., 2000] to 16 or 30°/s [Chawla et al., 1998, 1999]. This trend is consistent with the data presented in this study, which only depicts the lower part (<2.7°/s) of the tuning curve, and a point of interest for a future study would be to better define the entire curve.

If the  $\beta$ -band activity is acting as localized gating of cortical activity as part of a thalamocortical loop, it is interesting to note that there is not a complete loss of local power during stimulation. The ERD reflects a local loss in 15–30 Hz power of 10–12%, thus implying that the majority of the power within the band is still actively inhibiting other areas of cortex.

## CONCLUSIONS

The similarity in the  $\beta$ -band time-courses (ERD and poststimulus rebound) from different cortical regions (motor and visual cortex) suggests that this is a general phenomenon with inherent properties, which are applicable to the entire cortex rather than being specific to one system. A temporal correspondence between  $\beta$ -activity and BOLD has been shown previously by EEG/fMRI resting state studies. By using an activation-based study and the superior spatial resolution of MEG, we demonstrate a striking spatial colocalization of these two disparate phenomena (electromagnetically based oscillatory activity and blood flow based BOLD), which indicates that electrical effects in the  $\beta$ -band and the fMRI BOLD response are intimately related to each other and also to the neuronal activity that they each reflect. The uncoupling of amplitude modulation in the BOLD response and  $\beta$ -band oscillations highlights the complex relationship between neuromagnetic effects and hemodynamic effects giving rise to the BOLD response. The stimulus dependence of modulations in  $\beta$ -band power are largely consistent with a gating role for  $\beta$ -oscillations with no modulation of amplitude of desynchronization with either increasing stimulus duration, in the motor cortex, or increasing stimulus contrast, in the visual cortex. If the  $\beta$ -band activity is acting as localized gating of cortical activity as part of a thalamocortical loop, it is interesting to note that there is not a complete loss of local power during stimulation. The ERD

reflects a local loss in 15–30 Hz power of 10–12%, thus implying that the majority of the power within the band may still be actively inhibiting other areas cortex. This however requires further investigation as there is a modulation in the level of desynchronization with variations in drift frequency of the visual stimulus.

## REFERENCES

- Allison JD, Melzer P, Ding Y, Bonds AB, Casagrande VA (2000): Differential contributions of magnocellular and parvocellular pathways to the contrast response of neurons in bushy primary visual cortex (V1). *Visual Neurosci* 17:71–76.
- Bandettini PA, Wong EC, Hinks RS, Tikofsky RS, Hyde JS (1992): Time course EPI of human brain function during task activation. *Magn Reson Med* 25:390–397.
- Barnes GR, Hillebrand A (2003): Statistical flattening of MEG beamformer images. *Hum Brain Mapp* 18:14–30.
- Barnes GR, Hillebrand A, Fawcett IP, Singh KD (2004): Realistic spatial sampling for MEG beamformer images. *Hum Brain Mapp* 23:120–127.
- Bauer M, Oostenveld R, Peeters M, Fries P (2006): Tactile spatial attention enhances gamma-band activity in somatosensory cortex and reduces low-frequency activity in parieto-occipital areas. *J Neurosci* 26:490–501.
- Blackledge JM (2003): *Digital Signal Processing*. Chichester: Horwood.
- Born RT, and Bradley DC (2005): Structure and function of visual area MT. *Annu Rev Neurosci* 28:157–189.
- Brookes MJ, Gibson AM, Hall SD, Furlong PL, Barnes GR, Hillebrand A, Singh KD, Holliday IE, Francis ST, Morris PG (2005): GLM-beamformer method demonstrates stationary field, alpha ERD and gamma ERS co-localisation with fMRI BOLD response in visual cortex. *NeuroImage* 26:302–308.
- Brookes MJ, Mullinger KM, Stevenson CM, Morris PG, Bowtell R (2008): Simultaneous EEG source localization and artifact rejection during concurrent fMRI by means of spatial filtering. *NeuroImage* 40:1090–1104.
- Buckner RL, Andrews-Hanna JR, Schacter DL (2008): The Brain’s Default Network. *Anatomy, function and relevance to disease*. *Ann NY Acad Sci* 1124:1–38.
- Cassim F, Monaca C, Szurhaj W, Bourriez JL, Defebvre L, Derambure P, Guieu JD (2001): Does post-movement beta synchronization reflect an idling motor cortex? *NeuroReport* 12:3859–3863.
- Cheyne D, Bakhtazad L, Gaetz W (2006): Spatiotemporal mapping of cortical activity accompanying voluntary movements using an event-related beamforming approach. *Human Brain Mapp* 27:213–229.
- Courtemanche R, Fujii N, Graybiel AM (2003): Synchronous, focally modulated  $\beta$ -band oscillations characterize local field potential activity in the striatum of awake behaving monkeys. *J Neurosci* 23:11741–11752.
- Derrington AM, Lennie P (1984): Spatial and temporal contrast sensitivities of neurons in lateral geniculate nucleus of macaque. *J Physiol* 357:219–240.
- Eulitz C, Obleser J (2007): Perception of acoustically complex phonological features in vowels is reflected in the induced brain-magnetic activity. *Behav Brain Funct* 3:26.
- Fawcett IP, Barnes GR, Hillebrand A, Singh KD (2004): The temporal frequency tuning of human visual cortex investigated

- using synthetic aperture magnetometry. *NeuroImage* 1542–1553.
- Fox PT, Raichle ME (1984): Stimulus rate dependence of regional cerebral blood flow in human striate cortex, demonstrated by positron emission tomography. *J Neurophysiol* 51:1109–1120.
- Fox PT, Raichle ME (1986): Focal physiological uncoupling of cerebral blood flow and oxidative metabolism during somatosensory stimulation in human subjects. *Proc Natl Acad Sci USA* 83:1140–1144.
- Friston KJ, Fletcher P, Josephs O, Holmes A, Rugg MD, Turner R (1998): Event-related fMRI: Characterizing differential responses. *NeuroImage* 7:30–40.
- Gail A, Brinksmeier HJ, Eckhorn R (2000): Contour decouples gamma activity across texture representation in monkey striate cortex. *Cereb Cortex* 10:840–850.
- Glover GH (1999): Deconvolution of impulse response in event-related BOLD fMRI. *NeuroImage* 9:416–429.
- Hadjipapas A, Adjamian P, Swettenham JB, Holliday IE, Barnes GRM (2007): Stimuli of varying spatial scale induce gamma activity with distinct temporal characteristics in human visual cortex. *NeuroImage* 35:518–530.
- Hall SD, Holliday IE, Hillebrand A, Singh KD, Furlong PL, Hadjipapas A, Barnes GR (2005): The missing link: Analogous human and primate cortical gamma oscillations. *NeuroImage* 26:13–17.
- Heeger DJ, Ress D (2002): What does fMRI tell us about neuronal activity? *Nat NeuroSci Rev* 3:142–151.
- Henrie JA, Shapley R (2005): LFP power spectra in V1 cortex: The graded effect of stimulus contrast. *J Neurophysiol* 94:479–490.
- Joliot M, Ribary U, Llinas R (1994): Human oscillatory brain activity near 40 Hz coexists with cognitive temporal binding. *Proc Natl Acad Sci USA* 91:11748–11751.
- Jurkiewicz MT, Gaetz WC, Bostan AC, Cheyne D (2006): Post-movement beta rebound is generated in motor cortex: Evidence from neuromagnetic recordings. *NeuroImage* 32:1281–1289.
- Kisley MA, Cornwell ZM (2006): Gamma and beta neural activity evoked during a sensory gating paradigm: Effects of auditory, somatosensory and cross-modal stimulation. *Clin Neurophysiol* 117:2549–2563.
- Kwong KK, Belliveau JW, Chesler DA, Goldberg IE, Weisskoff RM, Poncelet BP, Kennedy DN, Hoppel BE, Cohen MS, Turner R, Cheng HM, Brady TJ, Rosen BR (1992): Dynamic magnetic resonance imaging of human brain activity during primary sensory stimulation. *Proc Natl Acad Sci USA* 89:5675–5679.
- Lachaux JP, Fonlupt P, Kahane P, Minotti L, Hoffmann D, Bertrand O, Baciau M. (2007) Relationship between task-related gamma oscillations and BOLD signal: New digits from combined fMRI and intracranial EEG. *Human Brain Mapp* 28:1368–1375.
- Laufs H, Krakow K, Sterzer P, Eger E, Beyerle A, Salek-Haddadi A, Kleinschmidt A (2003b) Electroencephalographic signatures of attentional and cognitive default modes in spontaneous brain activity fluctuations at rest. *Proc Natl Acad Sci* 100:11053–11058.
- Logothetis NK, Pauls J, Augath M, Trinath T, Oeltermann A (2001): Neurophysiological investigation of the basis of the fMRI signal. *Nature* 412:150–157.
- Malonek D, et al. (1997): Vascular imprints of neuronal activity: Relationships between the dynamics of cortical blood flow, oxygenation, and volume changes following sensory stimulation. *Proc Natl Acad Sci USA* 94:14826–14831.
- Malonek D, Grinvald A (1996): Interactions between electrical activity and cortical microcirculation revealed by imaging spectroscopy: Implications for functional brain mapping. *Science* 272:551–554.
- Mantini D, Perrucci MG, Del Gratta C, Romani GL, Corbetta M (2007): Electrophysiological signatures of resting state networks in the human brain. *Proc Natl Acad Sci* 104:13170–13175.
- Miller KJ, Leuthardt EC, Schalk G, Rao RPN, Anderson NR, Moran DW, Miller JW Ojemann JG (2007): Spectral changes in cortical surface potentials during motor movement. *J Neurosci* 27:2424–2432.
- Miller KJ, Weaver KE, Ojemann JG (2009): Direct electrophysiological measurement of human default network areas. *Proc Natl Acad Sci* 106:12174–12177.
- Muthukumaraswamy SD, Singh KD (2008): Spatiotemporal frequency tuning of BOLD and gamma band MEG responses compared in primary visual cortex. *NeuroImage* 40:1552–1560.
- Ogawa S, Lee TM, Kay AR, Tank DW (1990): Brain magnetic resonance imaging with contrast dependent on blood oxygenation. *Proc Natl Acad Sci USA* 87:9868–9872.
- Oishi N, Mima T, Ishii K, Bushara KO, Hiraoka T, Ueki Y, Fukuyama H, Hallett M (2007): Neural correlates of regional EEG power change. *NeuroImage* 36:1301–1312.
- Paradiso G, Cunic D, Saint-Cyr JA, Hoque T, Lozano AM, Lang AE, Chen R (2004): Involvement of human thalamus in the preparation of self-paced movement. *Brain* 127:2717–2731.
- Park HW, Ro YM, Cho ZH (1988): Measurement of the magnetic susceptibility effect in high-field NMR imaging. *Phys Med Biol* 33:339–349.
- Parkes LM, Bastiaansen MCM, Norris DG (2006): Combining EEG and fMRI to investigate the post-movement beta rebound. *NeuroImage* 29:685–696.
- Perez-Orive J, Mazor O, Turner GC, Cassenaer S, Wilson RI, Laurent G. (2002): Oscillations and sparsening of odor representations in the mushroom body. *Science* 297:359–365.
- Pfurtscheller G, Stancak A Jr., Neuper C (1996): Post-movement beta synchronization. A correlate of an idling motor area? *Electroencephalogr Clin Neurophysiol* 98:281–293.
- Ribary U, Ioannides A, Singh KD, Hasson R, Bolton JP, Lado F, Mogilner A, Llinas R (1991): Magnetic field tomography of coherent thalamocortical 40 Hz oscillations in humans. *Proc Natl Acad Sci USA* 88:11037–11041.
- Ritter P, Moosmann M, Villringer A (2009): Rolandic alpha and beta EEG rhythms' strength are inversely related to fMRI-BOLD signal in primary somatosensory and motor cortex. *Human Brain Mapp* 30:1168–1187.
- Robinson S, Vrba J. (1998): Functional neuroimaging: Synthetic Aperture Magnetometry. In: Yoshimoto T, Kotani M, Kuriki S, Karibe H, Nakasato N. (Eds.), *Recent Advances in Biomagnetism*. Tohoku Univ. Press, Sendai, Japan, pp. 302–305.
- Salmelin R, Hamalainen M, Kajola M, Hari R (1995): Functional segregation of movement-related rhythmic activity in the human brain. *NeuroImage* 2:237–243.
- Schnitzler A, Gross J (2005): Normal and pathological oscillatory communication in the brain. *Nat NeuroSci Rev* 6:285–296.
- Singh KD, Holliday IE, Furlong PL, Harding GFA (1997): Evaluation of MRI-MEG/EEG co-registration strategies using Monte

- Carlo simulation. *Electroencephalogr Clin Neurophysiol* 102: 81–85.
- Singh KD, Barnes GR, Hillebrand A, Forde EM, Williams AL (2002): Task-related changes in cortical synchronisation are spatially coincident with the haemodynamic response. *Neuroimage* 16:103–114.
- Smith SM (2002): Fast robust automated brain extraction. *Hum Brain Mapp* 17:143–155.
- Stancak A Jr., Pfurtscheller G (1995): Desynchronisation and recovery of beta rhythms during brisk and slow self-paced finger movements in man. *Neurosci Lett* 196:21–24.
- Swettenham JB, Muthukumaraswamy SD, Singh KD (2009): Spectral properties of induced and evoked gamma oscillations in human early visual cortex to moving and stationary stimuli. *J Neurophysiol* 102:1241–1253.
- Taniguchi M, Kato A, Fujita N, Hirata M, Tanaka H, Kihara T, Ninomiya H, Hirabuki N, Nakamura H, Robinson SE, Cheyne D, Yoshimine T (2000): Movement-related desynchronisation of the cerebral cortex studied with spatially filtered magnetoencephalography. *NeuroImage* 12:298–306.
- Toma K, Nagamine T, Yazawa S, Terada K, Ikeda A, Honda M, Oga T, Shibasaki H (2000): Desynchronisation and synchronization of central 20 Hz rhythms associated with voluntary muscle relaxation: a magnetoencephalographic study. *Exp Brain Res* 134:417–425.
- Tootell RB, Reppas JB, Kwong KK, Malach R, Born RT, Brady TJ, Rosen BR, Belliveau JW (1995): Functional analysis of human MT and related visual cortical areas using magnetic resonance imaging. *J Neurosci* 15:3215–3230.
- Winterer G, Carver FW, Musso M, Mattay V, Weinberger DR, Coppola R (2007): Complex relationship between BOLD signal and synchronization/desynchronisation of human brain MEG oscillations. *Human Brain Mapp* 28:805–816.
- Wrobel A (2000): Beta activity: A carrier for visual attention. *Acta Neurobiol Exp* 60:247–260.